Journal Pre-proof

A novel cholesterol conjugated fluorescence probe for Cu2+ detection and bioimaging in living cells

Jia Ting, Fu Mei, Zhang Mengyao, Qiu Jianwen, Zhu Hu, Gao Yong

PII: S1386-1425(19)30920-5

DOI: https://doi.org/10.1016/j.saa.2019.117530

Reference: SAA 117530

To appear in: *Spectrochimica Acta Part A: Molecular and Biomolecular Spectroscopy*

Received date: 31 July 2019

Revised date: 9 September 2019

Accepted date: 12 September 2019

Please cite this article as: J. Ting, F. Mei, Z. Mengyao, et al., A novel cholesterol conjugated fluorescence probe for Cu2+ detection and bioimaging in living cells, *Spectrochimica Acta Part A: Molecular and Biomolecular Spectroscopy*(2019), https://doi.org/10.1016/j.saa.2019.117530

A novel cholesterol conjugated fluorescence probe for Cu^{2+} detection and bioimaging in living cells

Jia Ting[1], Fu Mei[1], Zhang Mengyao[1], Qiu Jianwen[1], Zhu Hu[1,2], Gao Yong[1,2]*

(1. College of Chemistry and Materials Science, Fujian Normal University, Fuzhou 350007, China; 2. Fujian Provincial University Engineering Research Center of Industrial Biocatalysis, Fujian Normal University, Fuzhou, 350117, China)

Abstract

A cholesterol conjugated fluorescence probe **T** was designed and synthesized. The probe **T** can be used for recognition of Cu^{2+} by the absorption spectrum, fluorescence spectrum, and naked eyes respectively in aqueous solution. The cell imaging experiments showed that the probe has good membrane permeability and a huge potentiality for the detection of Cu^{2+} in living cells.

Keywords

Cholesterol; Fluorescence; Probe; Cu^{2+}; Bioimaging

1. Introduction

For organic living organisms, many transition metal ions play a vital role[1]. Copper as the third most abundant transition metal element in human body after iron and zinc plays an important role in physiological process[2]. As a catalyst cofactor, it plays a key role in the synthesis of many metal enzymes. Copper is distributed in all tissues and body fluids of the human body, and the highest copper content is found in the liver[3]. However, excessive Cu^{2+} can lead to neurasthenia, such as Alzheimer's disease, Wilson's disease and elicit uncontrolled Fenton oxidation which is the important reasons of cancerization[4-5]. Considering the multifaceted

physiology functions, many techniques have been reported for the detection of trace copper ions in biological systems, such as, atomic absorption spectrometry (AAS)[6], atomic fluorescence spectrometry (AFS)[7], ion-coupled plasma-mass spectroscopy (ICP-MS)[8] and high performance liquid chromatography (HPLC)[9]. However, these methods of copper determination require extraction and pre-concentration step before analysis, which is time-consuming and expensive[10-11]. Therefore, it is urgent to find a new analytical technique for the detection of copper ions in living organisms. Recently, fluorescent probes have been developed as highly sensitive, rapid, visual, lossless and inexpensive tools for copper determination in biology research[12]. These fluorescent probes have a significant fluorescence response to Cu^{2+} with specific selectivity and high sensitivity, but few of them can be used in biological samples by the lack of biocompatibility[13-14] and membrane permeability[15].

As a kind of biological amphiphile, cholesterol is an important component of mammalian cell membranes. It plays an indispensable role in regulating cell membrane properties in mammalian cells[16]. It is reported that cholesterol moiety can greatly improve the biocompatibility and membrane permeability of a drug delivery system.[17] But it is surprising that there are seldom reports about the utility of cholesterol in fluorescent probe[18].

After the first rhodamine-based copper ion fluorescent probe[19] was reported in 1997, rhodamine hydrazide has been considered as a typical framework to develop many copper ion fluorescent probes by utilizing the property of spirocyclic closed and ring-opened forms, which exhibits a “turn-on” signal response[20-24].

In this work, we designed and synthesized a novel cholesterol conjugated fluorescent Cu^{2+} probe **T** (Scheme1). Based on the homoousian of cholesterol with membrane lipids, we envisage that probe **T** should have better biocompatibility and membrane permeability.

On the other hand, recent studies have shown that cholesterol and its lipid regions composed of other lipid components of membranes are not only involved in the distribution of membrane proteins on the cell membrane surface but also play an important role in many cellular events such as cell signal transduction, immune response activation and substance transport.[25] A deep understanding of cholesterol metabolism is key toward developing efficient and targeted drugs for overcoming cholesterol-related disorders. Therefore, research for visualization of cholesterol in cells has caused widespread concern[26-27]. Interestingly, the probe **T** we designed can also be considered as visualized cholesterol by triggering with Cu^{2+}.

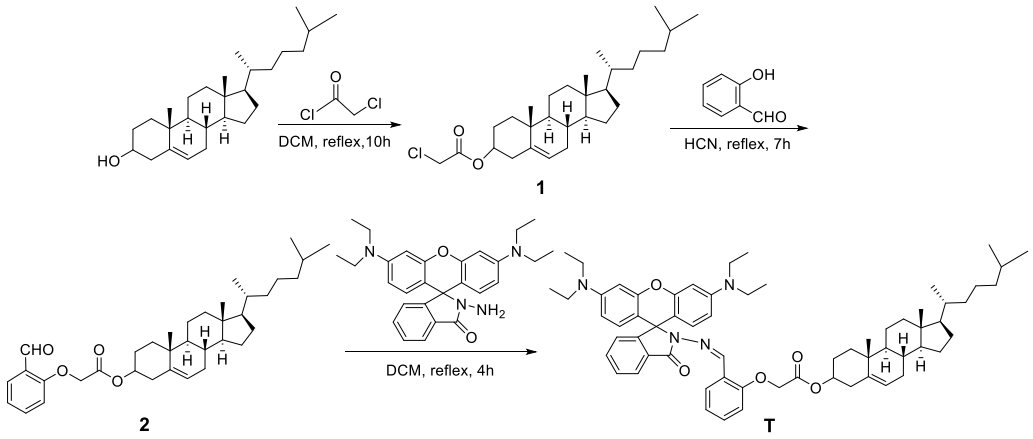

Scheme 1. The synthesis process of **T**

2. Experimental

2.1 Materials and physical methods

All reagents for synthesis were purchased from commercial suppliers and stored in a vacuum desiccator. They were used without further purification. The solutions of metal ions were prepared from their perchlorate salts. Tris-HCl buffer solutions (50 mM, pH=7.4) were prepared in deionized water. Fluorescence spectra were recorded on a RF-5310 PC Fluorescence Spectrometer. UV–visible spectra were recorded on a UV-1750UVspectrometer. ^{1}H NMR and ^{13}C NMR spectra were recorded on a VarianUnity-400 spectrometer operating at 400 MHz and 100 MHz, respectively. Chemical shifts are reported in ppm downfield from tetramethyl silane (TMS, δ scale) with the solvent resonances as internal standards. High-resolution mass spectra were conducted on a Bruker microTOF-QII ESI-MS. Cell image was

performed on Olympus FV1000-IX81 Fluorescence imager (100-fold oil mirror).

2.2 Synthesis of intermediate **1**

A solution of cholesterol (2.0718g, 36mmol) in DCM (50ml) was added chloroacetyl chloride (2.5mL) at room temperature. The reaction solution was heated to reflux for 10h. After the reaction was completed, the mixture was cooled to room temperature and washed with H_2O (30 mL×3). The organic phase was dried over anhydrous $MgSO_4$ and evaporated in vacuum. The crude product was further purified by column chromatography (Petroleum ether: DCM = 50:1) to afford intermediate **1**(1.2848g, 51.77%). ^{1}HNMR (400 MHz, $CDCl_3$, ppm) δ: 5.41(s, 1H, =CH), 4.05 (s, 2H, -CH_2CO-), 2.38 (d, 2H), 2.10-0.8(m, 19H), 0.69 (s, 3H, -CH_3). (Fig.S1)

2.3 Synthesis of intermediate **2**

Intermediate **1** (0.2972g, 0.64mmol), potassium carbonate (0.1838g, 1.33mmol) and potassium iodide (0.1077g, 0.64mmol) were combined in acetonitrile (10 mL) and stirred. Salicylaldehyde (0.2mL, 1.9mmol) was added dropwise. The reaction mixture was heated to reflux for 7h. The mixture was cooled and concentrated by evaporation under reduced pressure. The residue was dissolved in DCM (20mL) and was washed with H_2O (30 mL×3). The organic phase was dried over anhydrous $MgSO_4$ and the solvent was evaporated under reduced pressure, afforded

the intermediate **2** (0.3222g, 91.48%). ^{1}HNMR (400 MHz, $CDCl_3$, ppm) δ: 10.59(s, 1H, CHO), 7.88(d, 1H, ArH), 7.55(t, 1H, ArH), 7.10(t, 1H, ArH), 6.88(d, 1H, ArH), 5.37(s, 1H, =CH), 4.73 (s, 2H, -CH_2CO-), 2.38 (d, 2H,), 2.10-0,8(m, 19H), 0.65 (s, 3H, -CH_3). (Fig.S2)

2.4 Synthesis of **T**

Rhodamine hydrazide was synthesized according to the literature procedures [21]. Rhodamine hydrazide (0.2121g, 0.46mmol) was dissolved in absolute ethanol (20mL) and stirred. The intermediate **2** (0.3016g, 0.55mmol) in DCM (10mL) was added dropwise. The reaction mixture was heated to reflux for 4h. After cooling to room temperature, the reactant was stored for several days, and a white precipitate was formed. The precipitate was filtrated and dried in vacuum to afford **T** (0.2096g, 45.71%). ^{1}HNMR (400 MHz, $CDCl_3$, ppm) δ: 7.99(d, 2H, ArH), 7.88(d, 1H, ArH), 7.49(m, 2H, ArH), 7.20(m, 2H, ArH), 6.93(t, 1H, ArH), 6.73(d, 2H, ArH), 6.53(d, 2H, ArH), 6.43(d, 2H, ArH), 5.37(s, 1H, =CH), 4.73 (s, 2H, -CH_2CO-), 3.34(d, 8H, -CH_2-) 2.38 (d, 2H,), 2.10-0,8(m, 31H), 0.65 (s, 3H, -CH_3). (Fig.S3) ^{13}CNMR (100 MHz, $CDCl_3$, ppm) δ: 189.66, 168.39, 167.63, 164.78, 160.52, 157.78, 155.94, 153.94, 151.82, 148.83, 143.65, 140.83, 139.40, 135.72, 133.18, 132.45, 131.14, 130.83, 129.64, 128.85, 128.12, 126.59, 125.32, 124.14, 123.88, 122.90, 121.84, 113.57, 112.67, 107.96, 106.45, 97.89, 76.76, 75.61, 71.76, 66.96, 65.88, 56.79, 50.16, 50.03, 44.34, 42.33, 39.81, 37.96, 36.95, 36.21, 35.81, 31.93,

31.86, 29.73, 28.26, 28.03, 27.65, 24.32, 23.86, 22.85, 22.59, 21.11, 21.05, 19.42, 19.32, 18.75, 12.68, 11.89. (Fig.S4) HRMS (ESI) calcd. for $C_{64}H_{81}N_4O_5Na$[M+Na]: 1009.3417; found:1009.3478. (Fig.S5)

2.5 General procedure for spectra experiments

A stock solution of **T** (5×10^{-4}mol·L^{-1}) was prepared in DMF. The solution of **T** in the test system was then diluted to 1×10^{-5}mol·L^{-1} with DMF/Tris-HCl buffer solution (1:3, V/V). All fluorescence spectra are collected at an excitation wavelength of 510 nm (slit width: 2/2 nm).

2.6 Cell imaging

MCF-7 cells were incubated with 20μM **T** in DMSO/PBS (1:100, v/v) for 30 min at 37°C and 5% CO_2 and then washed with PBS three times. After incubating with 5μM of Cu^{2+} for 30 min at 37°C and 5% CO_2 and then the cells were washed with PBS three times again. Cell imaging of Cu^{2+} in MCF-7 cells was conducted by using a confocal fluorescence microscopy. The excitation light was excited at 559nm and the 575-620nm band was collected.

3. Results and discussions

3.1 Selectivity of the probe **T** to Cu^{2+}

As the introduction of amphipathic cholesterol, the first thing we want to know is the solubility of this new compound in aqueous solution. Absorption spectra were recorded from 200 to 800 nm for the solutions of **T** (10 μM) in a serious of different volume ratio of DMF and Tris-HCl

buffer. (Fig.S6) There are no absorption peak from 450 nm to 800 nm when the volume ratio of DMF and Tris-HCl buffer is 1:1, 1:2 or 1:3. It means the probe is soluble and stable in the solutions. But when the ratio is larger than 1:3, the absorptions are significantly enhanced. Based on that experiment, we selected the DMF/Tris-HCl buffer solution (1:3, V/V) as the solvent for **T** to do spectroscopic properties research.

The spectroscopic properties of probe **T** were primarily determined by the selectivity of the probe **T** to Cu^{2+} with UV-vis absorption and fluorescence spectra, respectively. As shown in UV-vis absorption spectrum (Fig.1), there was no absorption peak at 562nm for the probe **T**. After adding 2 equiv. amount of Cu^{2+}, the absorbance increased obviously at 562nm and the color changed from colorless to orange-red. But under the same conditions, the addition of 2 equiv. amount of K^{+}、Na^{+}、Ca^{2+}、Mg^{2+}、Zn^{2+}、Cd^{2+}、Mn^{2+}、Pb^{2+}、Fe^{3+} did not cause any absorption peak and color variation.

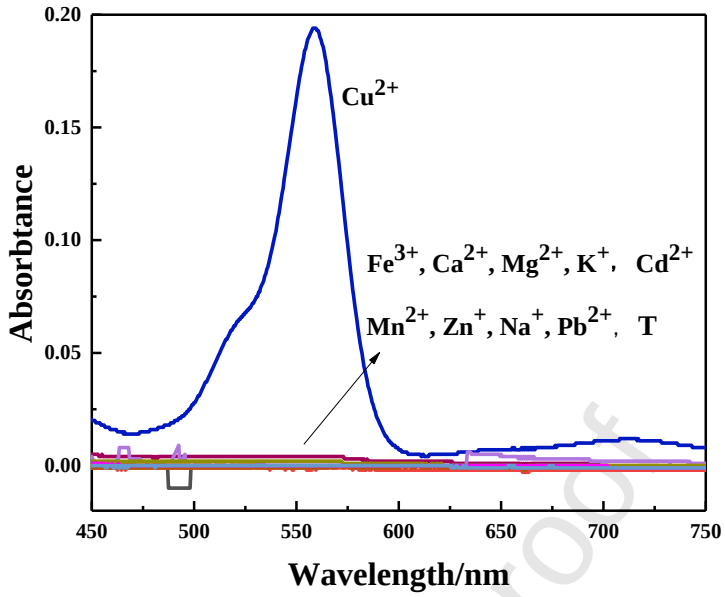

Fig.1.The UV-vis absorption spectra of probe **T**(10μM) in the presence and absence of different metal ions (20μM) in DMF/Tris-HCl (1:3, v/v)

As shown in the fluorescent spectrum (Fig.2), **T** itself had no significant fluorescence intensity. Once the probe was exposed to Cu^{2+}, a strong emission band appeared at 586nm accompanied by fluorescence enhancement. While other cationic solutions were added under the same conditions, the fluorescence spectra did not change significantly. The results show that probe **T** has good selectivity for Cu^{2+}, and the probe can be used as a naked eye chemical sensor for the detection of Cu^{2+}.

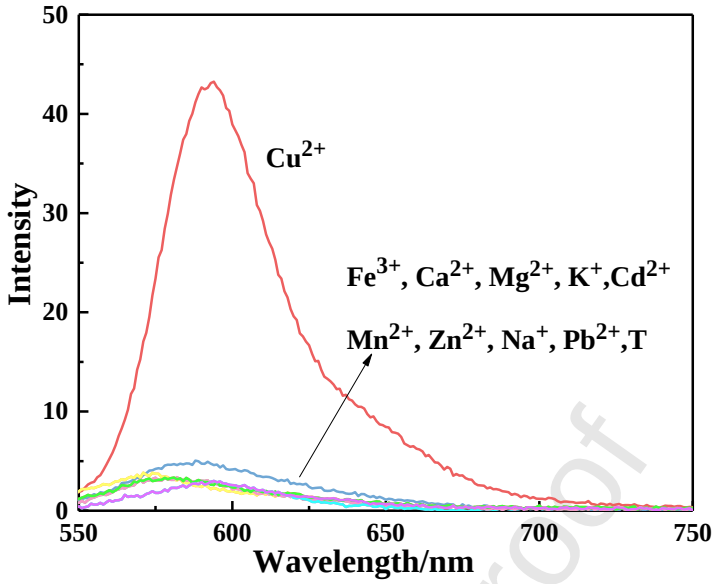

Fig.2. The fluorescent emission spectra of probe **T**(10μM) in the presence and absence of different metal ions (20 μM) in DMF/Tris-HCl (1:3, v/v).

3.2 The anti-interference of the probe T

The anti-interference of the probe to competing ions is very important for the practical application of a probe. So the anti-interference experiments were conducted with the common metal ions mentioned above, respectively. As shown in Fig.3, the probe **T** does not have obvious fluorescence in the presence of 10 equiv. interfering ions. After adding 3 equiv. Cu^{2+}, the fluorescence emission induced an obvious fluorescence intensity enhancement, while the other metal ions did not cause any discernible changes. This phenomenon indicates that these co-existent ions had a negligible interfering effect on Cu^{2+} sensing by **T**.

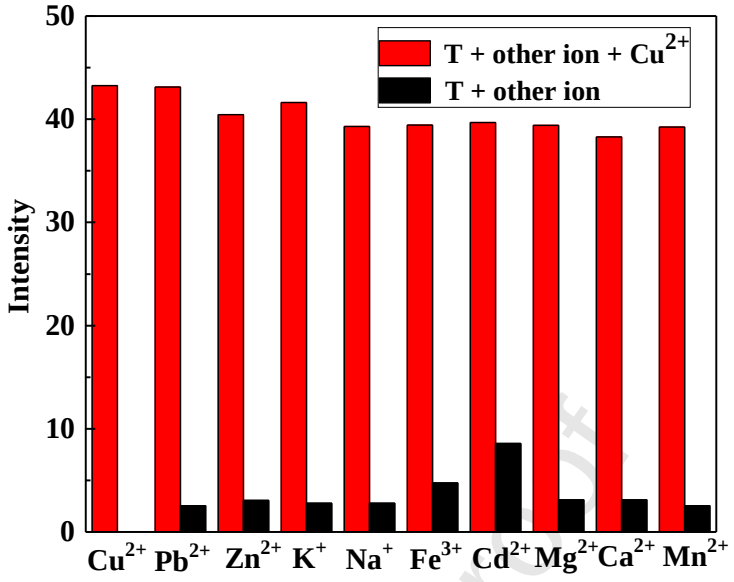

Fig.3. The Fluorescent emission spectra of probe **T**(10μM) in DMF/Tris-HCl (1:3, V/V) solution with the addition of 10 equiv. interfering ions and 3 equiv. copper ion.

3.3 UV-vis and fluorescent titration experiments

The spectroscopic properties of **T** at different concentrations of Cu^{2+} in DMF/Tris-HCl (1:3, V/V) solution were carried out. As shown in Fig.4, with the adding of Cu^{2+}a new absorption band appeared at 562nm and the absorbance increased with the increase of copper ion concentration.

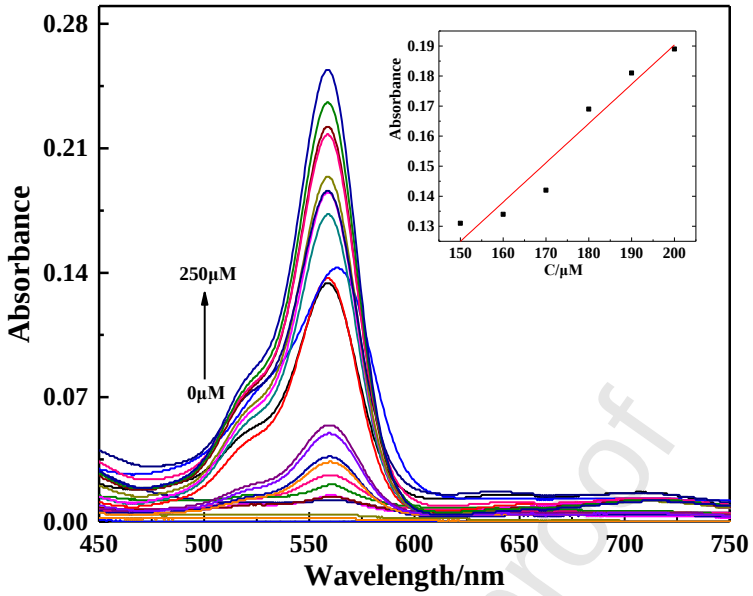

Fig.4. Absorption spectra of **T** (10 M) in DMF/Tris-HCl (1:3, V/V) upon addition of different amounts of Cu^{2+} ions.

Similarly, as shown in Fig.5, with the increase of copper ion concentration (0-250μM), a fluorescence emission band appeared at 586nm and the fluorescence intensity increased gradually with the adding of copper ion concentration. The fluorescence intensity has a good linear relationship with Cu^{2+} concentration ranging from 150 to 220μM (R^2=0.98462). At this condition, the detection limit of copper ion is 5.7μM. The above results indicate that the **T** could serve as a good fluorescent probe for Cu^{2+} detection.

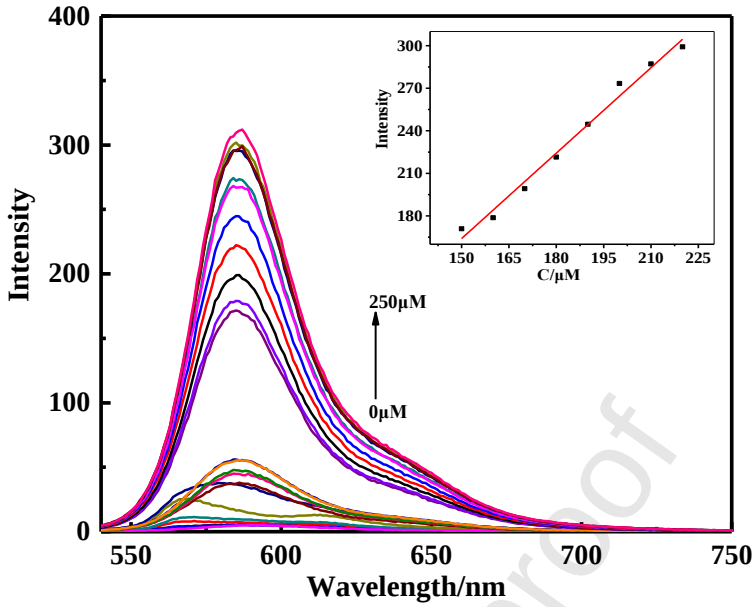

Fig.5. The fluorescent emission spectra of **T** (10 μM) in DMF/Tris-HCl (1:3, V/V) upon addition of different amounts of Cu^{2+} ions.

3.4 Reaction mechanism of T with Cu^{2+}

To explore the reaction mechanism of **T** with Cu^{2+}, the stoichiometry of the copper-**T** complex and reversibility of the reaction were investigated. Job's method for absorbance measurement was applied to determine the stoichiometry. The total concentration of the probe **T** and copper ions was immobilized as 2×10^{-4}M and the probe and copper ions were formulated to a concentration ratio of 10:0, 9:1, 8:2, 7:3, 6:4, 5:5, 4:6, 3:7, 2:8, 1:9. As shown in Fig.6, when the mole fraction of probe **T** reaches 0.5, the maximum absorbance value appears. This indicates a 1:1 stoichiometry of the Cu^{2+} to **T** in the complex.

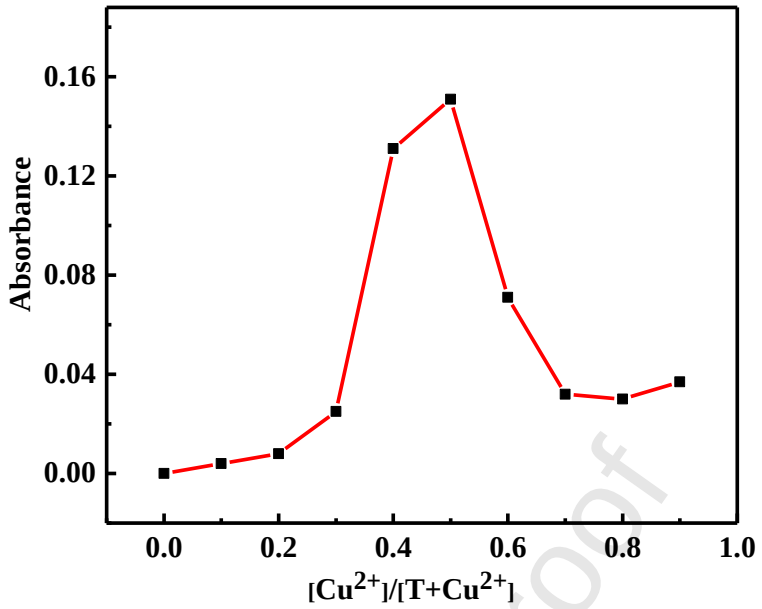

Fig.6 Job-plot of probe **T** for Cu^{2+} ion in DMF/Tris-HCl (1:3, V/V)

Reversibility experiments were conducted to indicate the possible mode of interaction between **T** and Cu^{2+}. As shown in Fig. S7, after the addition of 4 equiv. EDTA, the absorption peak at 562 nm decreased to the original pre-complex state. While re-adding 2 equiv. Cu^{2+} to the solution, the signals were almost recovered. The consecutive additions of EDTA and Cu^{2+} reveal that this cycle can be repeated at least three times. This indicates that the recognition of Cu^{2+} by probe **T** is based on reversible coordination.[28-29] According to the experiments and previously reported results[30-31], we assumed that the **T** most likely to chelate with Cu^{2+} ions to form a ring-opened complex (Fig. 7).

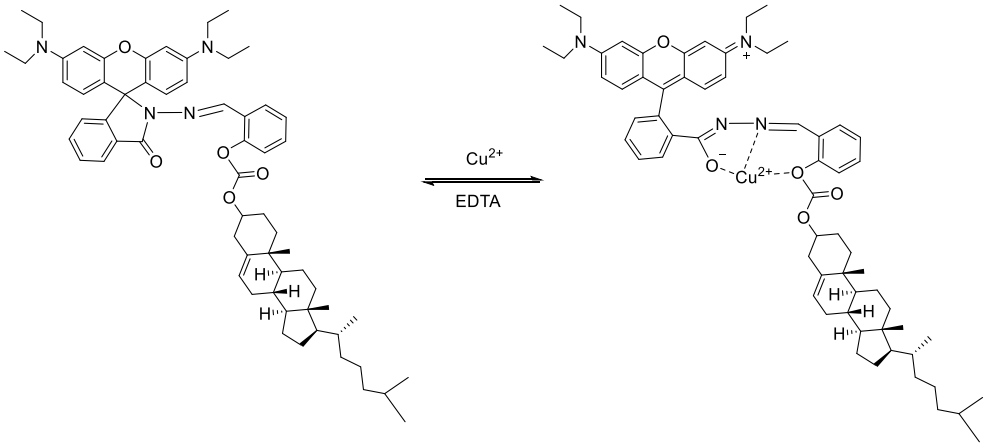

Fig. 7. Proposed mechanism for the detection of Cu^{2+} by **T**

3.5 Cell imaging

In order to verify the ability of the probe in bioimaging, probe **T** was used to detect Cu^{2+} in MCF-7 cells. From the bright field diagram (Fig.8A), it can be seen that the cell morphology is healthy in the confocal imaging experiment, indicating that the probe has excellent biocompatibility and low cytotoxicity. Observed under confocal fluorescence microscopy, there was significant fluorescence in the cell area. The overlay image of bright field and fluorescence shows that the fluorescent signal is in the cytoplasmic region, indicating that the probe has good cell membrane permeability. In contrast, the control sample didn't have fluorescence (Fig.8B). These results indicate that the probe has a huge potentiality for the detection of Cu^{2+} in biological cells.

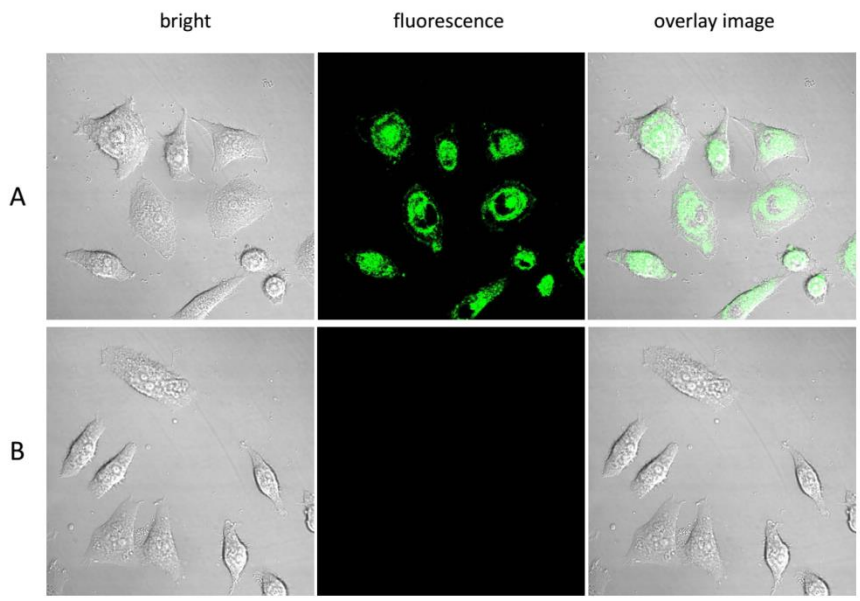

Fig.8. Fluorescence image of MCF-7 cells preloaded with **T** (20 μM) and incubated with (A) 5μM Cu^{2+}; (B) 0μM Cu^{2+}.

4. Conclusions

In summary, a novel cholesterol conjugated fluorescent probe **T** for Cu^{2+} was synthesized and characterized. The probe shows good selectivity and high sensitivity towards Cu^{2+} via a reversible binding mode over a wide range of tested metal ions. The cell image shows that the probe **T** has good cell membrane permeability and a huge potentiality for the detection of Cu^{2+} in biological cells. At the same time, the fluorescent image which was triggered by Cu^{2+} is also present the position of cholesterol. In this point, the probe **T** has potential use in tracking cholesterol in cells. This work is in progress by collaborators of our group and will be reported in due time.

Acknowledgments

This work was supported by the Natural Science Foundation of Fujian Province (No. 2018J01671, JK2017009).

References

[1] Y. M. Kuo, B. Zhou, D. Cosco, J. Gitschier, The copper transporter CTR1 provides an essential function in mammalian embryonic development, Proc. Natl. Acad. Sci. USA 98(2001), pp. 6836-6841.
[2] H. Liang, F. J. Chen, P. X. Xi, G. Q. Xie, Z. P. Li, Y. J. Shi, X. Min, A turn-on fluorescent chemosensor for Cu in aqueous media and its application to bioimaging, Dyes Pigments, 90(2011), pp.265-268.
[3] I. Bremner, Involvement of metallothionein in the hepatic metabolism of copper, J. Nutr. 117(1987), pp.19-29.
[4] A.I. Bush, C. L. Masters, R. E. Tanzi. Copper, beta-amyloid and Alzheimer's disease: tapping a sensitive connection, Proc. Natl. Acad. Sci. USA100(2003), pp.11193-11194.
[5] Y. Xiao, Q. X. Zhai, G. Wang, Metabolomics analysis reveals heavy metal copper-induced cytotoxicity in HT-29 human colon cancer cells, Rsc Adv. 6(2016), pp.78445-78456.
[6] M. Ghaedi, F. Ahmadi, A. Shokrollahi, Simultaneous preconcentration and determination of copper, nickel, cobalt and lead ions content by flame atomic absorption spectrometry, J. Hazard. Mater. 142(2007), pp.272-278
[7] L. He, X. F. Zhu, L.Wu, Determination of trace copper in biological samples by on-line chemical vapor generation-atomic fluorescence spectrometry, Atom. Spectrosc. 29(2008), pp.93-98.
[8] L. X. Feng, J. Wang, H. M. Li, A novel absolute quantitative imaging strategy of iron, copper and zinc in brain tissues by isotope dilution laser ablation ICP-MS, Anal. Chim. Acta 984(2017), pp.66-75.
[9] J. D. Peng, S. P. Liu, C. Y. Deng, Separation and determination of trace amounts of aluminium(III), vanadium(V), iron(III), copper(II) and nickel(II) with CALKS and PAR by RP-HPLC, Anal. Sci. 21(2005), pp.259-262.
[10] Y. Fang, Y. Zhou, Q. Q. Rui, C. Yao, Rhodamine–ferrocene conjugate chemosensor for selectively sensing copper(II) with multi signals: chromaticity, fluorescence, and electrochemistry and its application in living cell imaging, Organometallics 34(2015), pp.2962-2970.
[11] Z. Yang, M. Y. She, J. Zhang, X. X. Chen, Y. Y. Huang, H. Y. Zhu, P. Liu, J. L. Li, Z. Shi, Highly sensitive and selective rhodamine Schiff base “off-on” chemosensors for Cu^{2+} imaging in living cells, Sensor. Actuat. B. 176 (2013), pp.482-487.
[12] V. Stefan, R. Martina, Opportunities in multidimensional trace metal imaging: Taking copper associated disease research to the next level, Anal. Bioanal. Chem. 405(2013), pp.1809-1820.

[13] X. X. Li, Z. H. Qing, Y. N. Li, Natural peptide probe screened for high-performane fluorescent sensing of copper ion: especially sensitivity, rapidity, and environment- friendliness, ACS Omega 4(2019), pp.793-800.
[14] J. J. Guo, H. X. Huang, M. J. Zhou, Quantum dots-doped tapered hydrogel waveguide for ratiometric sensing of metal ions, Anal. Chem. 90(2018), pp.12292-12298.
[15] B. L.Yan, R. Sun, J. F. Ge, Synthesis and application of a full water-soluble and red-emitting chemosensor based on phenoxazinium for Copper(II) ions, Chin. J. Chem. 30 (2012), pp. 2303-2308.
[16] F. R. Maxfield, I. Tabas, Role of cholesterol and lipid organization in disease, Nature 438 (2005), pp.612-621.
[17] H. R. Leticia, Y. Zhang, B. M. Teo, Cholesterol-a biological compound as a building block in bionanotechnology, Nanoscale, 5(2013), pp.89-109.
[18] S. Iyoshi, M. Taki, Y. Yamamoto, Development of a cholesterol-conjugated fluorescent sensor for site-specific detection of zinc ion at the plasma membrane, Org. Lett.13(2011), pp.4558-4561.
[19] V. Dujols, F. Ford, A. W. Czarnik, A long-wavelength fluorescent chemodosimeter selective for Cu(II) ion in water, J. Am. Chem. Soc.119(1997), pp.7386-7387.
[20] L. F. Zhang, J. L. Zhao, X. Zeng, L. Mu, X. K. Jiang, M. Deng, J. X. Zhang, G. Wei, Tuning with pH: The selectivity of a new rhodamine B derivative chemosensor for Fe^{3+} and Cu^{2+}, Sensor. Actuat. B-Chem. 160(2011), pp. 662-669.
[21] Y. Xiang, A. J. Tong, P. Y. Jin, Y. Ju, New fluorescent rhodamine hydrazone chemosensor for Cu(II) with high selectivity and sensitivity. Org. Lett. 8(2006), pp.2863-2866.
[22] Z. H. Xu, L. Zhang, R. Guo, T. H. Xiang, C. Z. Wu, Z. Zhi, F. L. Yang. A highly sensitive and selective colorimetric and off-on fluorescent chemosensor for Cu^{2+} based on rhodamine B derivative. Sensor. Actuat. B-Chem. 156(2011), pp.546-552.
[23] L. Yuan, W. Y. Lin, B. Chen, Y. N. Xie, Development of FRET-based ratiometric fluorescent Cu^{2+} chemodosimeters and the applications for living cell imaging, Org. Lett. 14(2012), pp. 432-435.
[24] M. Tian, H. He, B. B. Wang, A reaction-based turn-on fluorescent sensor for the detection of Cu(II) with excellent sensitivity and selectivity: Synthesis, DFT calculations, kinetics and application in real water samples, Dyes. Pigments 165(2019), pp.383-390.
[25] S. K. Andrey, K.Remy, Fluorescent probes for lipid rafts: from model membranes to living cells, Chem. Bio. 21(2014), pp.97-113.
[26] M. H. ltta-Vuori, R. L. Uronen, J. Repakova, BODIPY-Cholesterol: A new tool to visualize sterol trafficking in living cells and organisms, Traffic 9(2008), pp.1839-1849.
[27] S. Erdinc, B. C. Fatma, S. Falk, A comparative study on fluorescent cholesterol analogs as versatile cellular reporters, J. Lipid Res. 57(2016), pp.299-309.
[28] Y. Zhou, F. Wang, Y. M. Kim, Cu^{2+}-Selective ratiometric and “off-on” sensor based on the rhodamine derivative bearing pyrene group, Org. Lett. 2009, 11(19):4442-4445.
[29] Y. Yang, C. Y. Gao, T. T. Li, A tetraphenylethene-based rhodamine hydrazone chemosensor for colorimetric and reversible detection of Cu^{2+}, ChemistrySelect 1 (2016), pp.4577-4581.
[30] J. Wang, Q. Yang, H. Song, A fluorescent probe of N′-formyl-rhodamine B hydrazide: structure and spectral properties of protonation behavior, Org. Biomol. Chem. 10(2012), pp.7677–7680.

[31] M. Dong, T. H. Ma, A. J. Zhang, A series of highly sensitive and selective fluorescent and colorimetric “off-on” chemosensors for Cu(II) based on rhodamine derivatives, Dyes. Pigments 87(2010), pp.164-172.

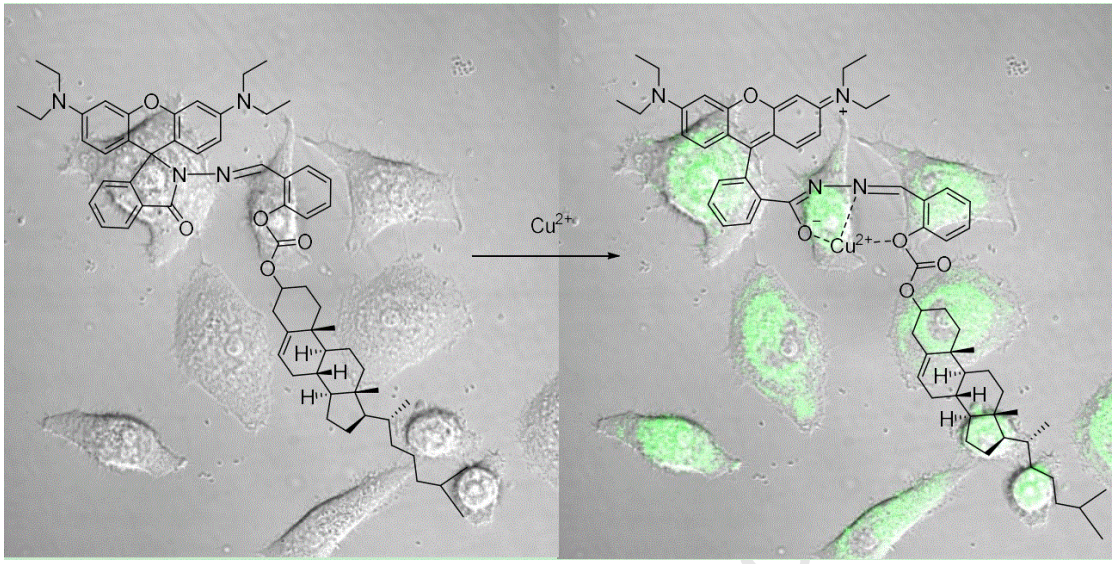

Graphical abstract

Highlights

- A novel cholesterol conjugated fluorescence probe **T** was designed and synthesized.
- The probe **T** exhibited a selective and sensitive response to Cu^{2+} in aqueous solution.
- The cell imaging experiments exhibited that the probe has good membrane permeability and huge potentiality for the detection of Cu^{2+} in living cells.